Polymer 321 (2025) 128144

Contents lists available at ScienceDirect

Polymer

journal homepage: www.elsevier.com/locate/polymer

Lamellar thickness of the polypropylene matrix determines surface induced nucleation of polyethylene droplets in immiscible blends

Leire Sangroniz [a,b,**], Enrico Carmeli [c], Lada Vukusic [c], Velichko Hristov [c], Martina Galatini [a], Davide Tranchida [c,***], Dario Cavallo [a,*]

[a] Department of Chemistry and Industrial Chemistry, University of Genova, Via Dodecaneso 31, 16146, Genova, Italy
[b] POLYMAT and Department of Polymers and Advanced Materials: Physics, Chemistry and Technology, Faculty of Chemistry, University of the Basque Country UPV/EHU, Paseo Manuel de Lardizábal, 3, 20018, Donostia-San Sebastián, Spain
[c] Borealis Polyolefine GmbH, Innovation Headquarters, St. Peterstrasse 25, 4021, Linz, Austria

ARTICLE INFO

Keywords:
Crystallization
Polymer blends
Surface nucleation
Self-nucleation
Epitaxy

ABSTRACT

Polyethylene (PE)/polypropylene (PP) blends have attracted much attention since they offer interesting physical properties, including intriguing crystallization behaviour. When PE minority phase is dispersed as droplet in PP matrix, we have recently proved that PP can induce surface induced nucleation of polyethylene. This occurs due to epitaxy, and is detected by measuring an increase of PE crystallization temperature upon varying the crystallization temperature of PP via self-nucleation. However, so far the role of the microstructure of PP substrate on this peculiar nucleation process has not been addressed. To gain insights on this issue PP with varying content of 2,1- erythro regiodefects or ethylene comonomer has been employed to tune the microstructure of the blend's matrix. Surface induced nucleation is investigated upon modifying the PP matrix morphology via self-nucleation. The modification of the nanoscale morphology of the matrix has been analysed with Small Angle X-ray Scattering (SAXS), allowing to determine the crystalline lamellar thickness. The increase in the crystallization temperature of PP matrix results in a thickening of the lamellae, which in turns enhances the surface induced nucleation of PE phase, as reflected by an increase in the crystallization temperature of PE. A clear correlation between the crystallization temperature of PE and the crystalline lamellar thickness of PP is found. In general, nucleation of PE is promoted by thicker PP lamellae, but surprisingly it can also occur (with lower efficiency) on PP lamellae that are thinner than the average lamellar thickness of the nucleating PE.

1. Introduction

Polymer crystallization commonly occurs via two steps, i.e., nucleation and crystal growth. When a polymer is cooled from the melt first some nuclei are formed (primary nucleation) and then the growth of the nuclei into 3-D macroscopic crystals follows [1–3]. Two types of nucleation are distinguished: homogeneous and heterogeneous nucleation [4–6]. The latter occurs on the surface of the heterogeneous material present in the polymer melt. In this process a lower energy barrier has to be overcome, with respect to homogeneous nucleation, resulting in nucleation at lower supercooling. This is the most usual case in polymers, since they contain several heterogeneities/impurities, such as catalytic residues. Homogeneous nucleation instead occurs when the nucleus is formed in the bulk of the phase, due to the random fluctuation of density of the polymer melt. If the nucleus reaches a crystallization temperature-dependent critical size, it will be stable and able to trigger the growth of the crystal, otherwise it will revert back to the melt phase. Homogeneous nucleation is unusual in bulk polymers since high undercoolings are required for this process to occur.

The study of the nucleation step in polymers is challenging since it is difficult to separate it from the growth stage. A suitable strategy to study nucleation is to divide the polymer in micro- or nano-domains in such a way that the nucleation step becomes the rate limiting process [7,8]. In fact, once the nucleation of the polymer has occurred, the growth within

---

This article is part of a special issue entitled: IDMPC2024 published in Polymer.
* Corresponding author.
** Corresponding author.
*** Corresponding author.

E-mail addresses: Davide.Tranchida@borealisgroup.com (D. Tranchida), dario.cavallo@unige.it (D. Cavallo).

https://doi.org/10.1016/j.polymer.2025.128144
Received 29 November 2024; Received in revised form 30 January 2025; Accepted 8 February 2025

the domain takes place in a very short time due to the limited domain size. So, the growth time can be considered to be negligible with respect to that required for nucleation.

An example of application of this strategy is blending two immiscible polymers, with the minority phase being a semicrystalline polymer [9, 10]. Under the appropriate composition and conditions it is possible to obtain a droplet-in-matrix morphology. Given the micro- or submicro-scale range of the droplets, nucleation is the rate limiting step of the overall crystallization kinetics of the dispersed phase. Nucleation of the droplets which are free of nucleating impurities can occur in the bulk (homogeneous nucleation) or at the interface with the matrix. The surface induced nucleation is a special case of heterogeneous nucleation and it can happen in contact with a solid or molten polymer interface. When the nucleation of a polymer occurs onto the surface of a second semicrystalline polymer, epitaxy can be in place if there is some extent of matching between the crystalline lattices of the two polymers. This is the case of polypropylene/polyethylene blends.

Indeed, PP and PE can be considered a model system to study epitaxy. This system has attracted a lot of attention, carrying out significant research to understand the physics behind this phenomena [11–17]. Analysing PE crystallization onto oriented PP films it has been proved that PE chains align in parallel along the methyl group rows provided by the PP. The distance between adjacent methyl groups is 0.505 nm in the (101) direction matching the distance between PE chains in the (100) plane, 0.494 nm. Therefore, PE chains crystallize forming a 50° angle with PP chain axis [11–16]. Yan et al. investigated oriented films of PP and PE proving that epitaxial crystallization depends on the lamellar thickness of iPP and PE crystals. They found no epitaxial relationship between the PE and the PP substrate when the lamellae of PP are thinner than the PE lamellae. The authors explain this phenomenon considering that PE/PP epitaxy depends on both the crystallographic matching and the secondary nucleation process. Detailed studies of PP/PE systems have shown that the crystallization rate and crystallization temperature impact the epitaxial growth. By studying several PE grades Yan et al. found that in the case of PP/PE films, there is a critical thickness of PE epitaxial layer on PP surface, which is inversely related to the PE density. From a more applied point of view, some works have shown that epitaxy improves the mechanical performance and processing methods to obtain well defined structures have been investigated [18–21]. Indeed, it is possible to obtain epitaxial growth of HDPE onto iPP employing dynamic packing injection moulding. The epitaxial growth depends on the relative amount of each phase, being the prevailing mechanism for PP 80 %/HDPE 20 % blends [18]. The epitaxial growth improves the mechanical performance due to the bridging effect between the amorphous phase of one polymer with the crystalline lamellae of the other polymer [20].

A novel strategy to study polymer-on-polymer nucleation kinetics have been developed by our group recently, based on the study of immiscible binary blends of semicrystalline polymers with droplet-in-matrix morphology [9,10]. The method consists in injecting self-nuclei or self-seeds in a controlled way in the matrix polymer, applying a self-nucleation procedure. With this method the crystallization temperature of the matrix increases. The relationship between the crystallization temperature of both matrix and dispersed phase is investigated to determine the nature of nucleation. The increase of the crystallization temperature (T_c) of the matrix results in a modification of the crystalline morphology (variation in the thickness of crystalline lamellae) which could promote the nucleation of the droplets leading to an increase of the T_c of the dispersed phase. This method is only suitable when the dispersed phase has a lower melting temperature than the one of the matrix.

Taking advantage of this procedure we proved that self-nucleation of PP promotes the surface nucleation of PE droplets in immiscible binary blends. PP-induced surface nucleation is more efficient than the nucleation provided by polyethylene self-nuclei themselves, which indicates a supernucleation effect [9]. More recently, we have studied how the regularity of PE chain can affect epitaxial crystallization [22]. The regularity of PE chains impact the surface nucleation of PE droplets on the PP matrix. The more regular chain structure of high density polyethylene (HDPE) shows a more efficient nucleation than linear low density polyethylene (LLDPE). For low density polyethylene (LDPE), which consists of highly branched chains, there is no surface nucleation. Thus, there is a minimum critical crystallizable sequence length of PE for the effective epitaxial matching between PE chains onto PP crystals. The irregularities (branches or comonomer units) do not allow the PE chains to align in the valleys formed by the methyl groups of the PP preventing an efficient nucleation.

Although PP/PE blends have been thoroughly investigated there are still some knowledge gaps that should be addressed considering the relevance of this system in industry. One of the unknown aspects is the role of PP matrix on the epitaxial crystallization of PE droplets on the matrix surface. In this work we take advantage of our novel procedure to ascertain how the regiodefects or the presence of comonomer in PP matrix can affect the surface nucleation of PE. For that, we have studied several PP/PE droplet-in-matrix blends with varying content of defects in the PP phase. Self-nucleation of PP has been carried out to quantify the extent of the surface nucleation effect, and its relationship with the PP matrix lamellar thickness has been explored studying the materials by Small Angle X-ray Scattering (SAXS).

2. Experimental section

2.1. Materials

All the materials were provided by Borealis Polyolefine GmbH. Polyethylene with density 935 kg/m^3 and a short chain branches of 15/kCH$_2$ was always employed as the minor phase in the blends. Several PP grades were used, including PP containing regiodefects and ethylene comonomer. In particular the employed PP were: highly isotactic PP with 98 mmmm % (mmmm indicates the content of stereodefects), PP with 1 % of 2.1e regiodefect and PP with 2.1 and 4.6 wt% of ethylene (C2) comonomer. The melt flow rate (MFR) for the neat materials is shown in Table S1, Supporting Information. 2.1e regiodefects are introduced in PP chains during polymerization, indeed regio or stereo defects can be generated. When olefin addition occurs as head-to-head regio 2,1-erythro defects are introduced. Those defects interrupt the regularity of the chain impacting thermal and physical properties [23, 24].

2.2. Blending

PP/PE blends were prepared in 80/20 wt% ratio by melt-mixing. The polymers have been melt-mixed for 10 min in an internal batch mixer HAAKE PolyLab by Thermo Fisher. The rotor speed was 50 rpm and the mixer barrel temperature was set to 180 °C. The composition and codes of the prepared blends are displayed in Table 1. In the sample code, the letter *r* stands for the amount of regiodefects, the letter *c* for the ethylene comonomer content. The number after each letter indicates the weight percentage of the defect. The samples r0.2c0, r0.4c0 and r0.6c0 have been prepared by blending in different proportions the r0c0 and r1c0

Table 1
Code and characteristics of the investigated PP/PE 80/20 wt% blends.

Code	r 2.1e %	c C2 wt%
r0c0	0	0
r1c0	1	0
r0c4.6	0	4.6
r0c2.1	0	2.1
r0.2c0	0.2	0
r0.4c0	0.4	0
r0.6c0	0.6	0

polypropylenes.

2.3. Scanning electron microscopy (SEM)

The morphology of the blends was studied employing SEM. The samples were first prepared in the Differential Scanning Calorimetry (DSC) applying the appropriate self-nucleation procedure with selected self-nucleation temperatures (T_s). Then the polymers were cut with a Leica EMUC7 microtome at −100 °C. Subsequently, they were etched using a 1 % $KMnO_4$ in 85 % H_2SO_4 solution for 15 min. Afterwards the samples were rinsed with deionized water for 10 min, and stirred in a 30 % H_2O_2 solution for 10 min. Finally, the etched samples were rinsed in deionized water and with acetone. The samples were then coated with Pt employing a Quorum Q150T S plus sputter coater and the images were acquired with a ThermoFischer Apreo SEM.

2.4. Differential Scanning Calorimetry (DSC)

The thermal properties of the blends were investigated using a DSC 250 from TA Instrument connected to an intracooler RCS90. The equipment was calibrated employing an Indium standard. All the measurements were performed in a nitrogen atmosphere, with a flow of 50 mL/min. Aluminium pans with 6–7 mg of material were prepared to carry out the experiments.

2.4.1. Non-isothermal experiments

To assess the thermal properties non-isothermal measurements were carried out by heating the materials to 200 °C at 10 °C/min, to ensure that the thermal history was removed. After spending 5 min at 200 °C, the material was cooled down to 0 °C at 10 °C/min, and it was heated again at 10 °C/min to record the melting behaviour of the polymer.

2.4.2. Self-nucleation experiments

The self-nucleation behaviour of the materials was studied employing the method developed by Fillon et al. [25–27] First the thermal history is removed by heating the material to 200 °C, see Fig. 1. After spending 5 min at 200 °C, the material is cooled down to 0 °C to obtain a standard crystalline state. Then the material is heated to the selected self-nucleation temperature, T_s, adequate for the self-nucleation study of the PP matrix. The sample is kept at this T_s temperature for 5 min and then it is cooled down to 0 °C. After this step the material is eventually heated to 200 °C. The heating and cooling scans have been performed at 10 °C/min. To determine the temperature range corresponding to each self-nucleation domain the cooling scan from T_s (a) and the subsequent heating scan (b) are analysed, see Fig. 1.

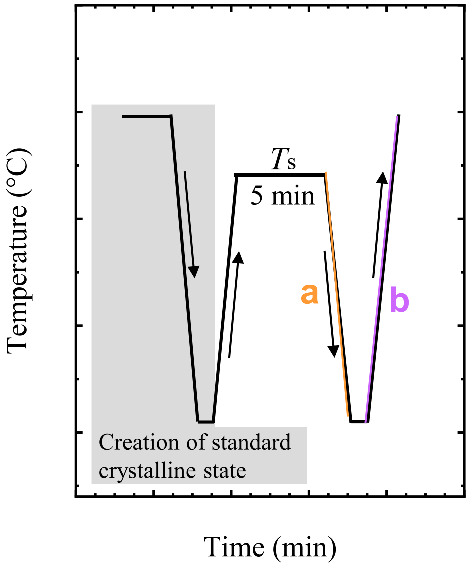

Fig. 1. Self-nucleation thermal procedure. The cooling scan from T_s (a) and the subsequent heating scan (b) are analysed to determine the *self-nucleation Domains* of the samples.

2.5. Small-angle X ray scattering

The lamellar thickness of the materials was determined by Small-Angle X-ray Scattering. The materials were measured at the BM26 beamline of the European Synchrotron Facility, ESRF France. The measurements were carried out employing a 12 keV X-ray source and a Pilatus 1 M detector with a sample-detector distance of 2.95 m. The raw data were integrated via the software Bubble, obtaining the scattered intensity as a function of the scattering vector, q, $q = (4\,\pi\,\sin\theta)/\lambda$ being 2θ the scattering angle and λ the wavelength [28–30]. The q-range was previously calibrated employing silver behenate as reference. The sole PP matrix was studied instead of the blends, since in the blends overlapping of PE and PP long period might occur, preventing the accurate determination of the PP matrix long period. As PE is the minor phase and it crystallizes after PP, it is assumed that it does not affect the lamellar morphology of the PP matrix phase in the blends. Thus, the SAXS data of the neat PP are considered as representative of those of the PP in the blends. The effect of PP self-nucleation temperature on the long period was assessed by studying materials that were previously prepared in the DSC according to the SN procedure at selected T_s.

2.6. Wide-Angle X ray scattering

The crystallinity degree of the materials and the crystalline structure was studied by Wide-Angle X-ray Scattering (WAXS). A Rigaku Mini-Flex600 diffractometer was employed with a Rigaku D/teX Ultra detector. CuKα was employed as X ray sourced filtered by Ni. A preliminary self-nucleation procedure without the last heating step was applied to the samples in the DSC to study the effect of the self-nucleation temperature on the crystalline state.

3. Results and discussion

3.1. Morphology of the blends

The binary PP/PE blends have been analysed by SEM to ascertain the morphology and the size of the droplets, after applying the self-nucleation procedure at a certain T_s. In all cases a droplet matrix morphology is observed with PE minority phase forming dispersed droplets (Fig. 2). The images indicate that the size of the droplets does not vary significantly with the type of PP matrix studied. In Table 2 the number average diameter of the droplets is displayed for a selection of the blends. Only slight variations are observed. The blends with an amount of regiodefects between 0 and 1 % are not displayed, but they are expected to have a morphology similar to that of the r0c0 and r1c0 blends. The results indicate that the incorporation of few regiodefects or comonomer does not impact in a significant way the blend morphology. Given the obtained similar droplet size, possible differences in the thermal behaviour between blends can be related to the characteristics of the PP matrix alone, rather than to differences in the morphology.

3.2. Non isothermal crystallization

Non-isothermal DSC experiments were performed to analyse the thermal properties of the blends, see Fig. 3. During the cooling scan most of the blends exhibit a single crystallization peak, which implies that simultaneous crystallization of PP and PE phases occur, i.e., a superposition of the crystallization processes of both polymers. The DSC scans of neat polymers are shown in SI (Fig. S1) and the melting and crystallization temperature are included in Table S2. For some of the blends such as r0c0, r0.2c0 or r0.4c0, a lower temperature shoulder can be

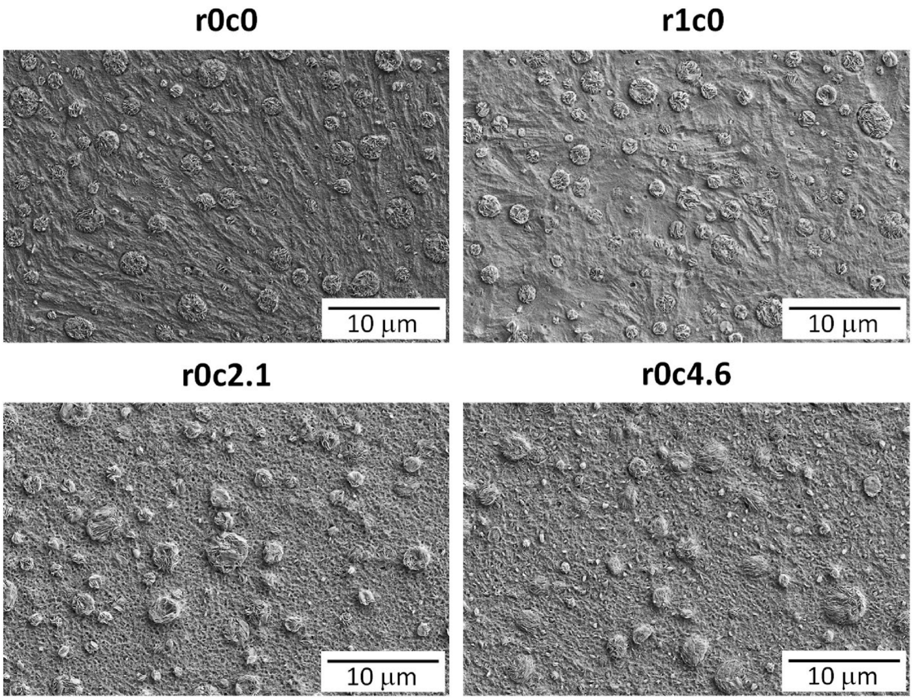

Fig. 2. SEM images of a selection of the studied blends after cooling to room temperature from specific T_s in DSC: r0c0 at 158 °C, r1c0 at 150 °C, r0c2.1 at 159 °C and r0c4.6 at 153 °C.

Table 2
Number average diameter (d_n) of the PE droplets in the different blends.

Blend	d_n (μm)
r0c0	1.34
r1c0	1.44
r0c2.1	1.52
r0c4.6	1.16

distinguished in the crystallization peak, which is attributed to the crystallization of the polyethylene phase. By increasing the amount of regiodefects there is a shift of the main T_c (related to the PP phase) to smaller values, as could be expected [31,32]. Similarly, when the ethylene comonomer is introduced in the PP chains lower crystallization temperatures are obtained [33].

The subsequent heating scans show two melting peaks, the one around 125 °C corresponds to the melting of PE and the second one ranging from 145 to 165 °C to the melting of the PP phase. There is a significant reduction of the melting temperature (T_m) of the PP phase with increasing the regiodefects content or introducing a comonomer, which is related with the formation of thinner crystalline lamellae upon previous crystallization. Instead, the melting temperature of the PE phase does not vary significantly with changing the PP matrix type, being the differences within 1 °C.

In the case of r0.2c0, r0.4c0 and r0.6c0 in which two polypropylene have been blended, considering that regiodefects are incorporated in the chain with extreme regularity there is minimum possible segregation and effects of non-random distributions. Indeed, the DSC results do not provide any sign of segregation of two PP types. As has been mentioned,

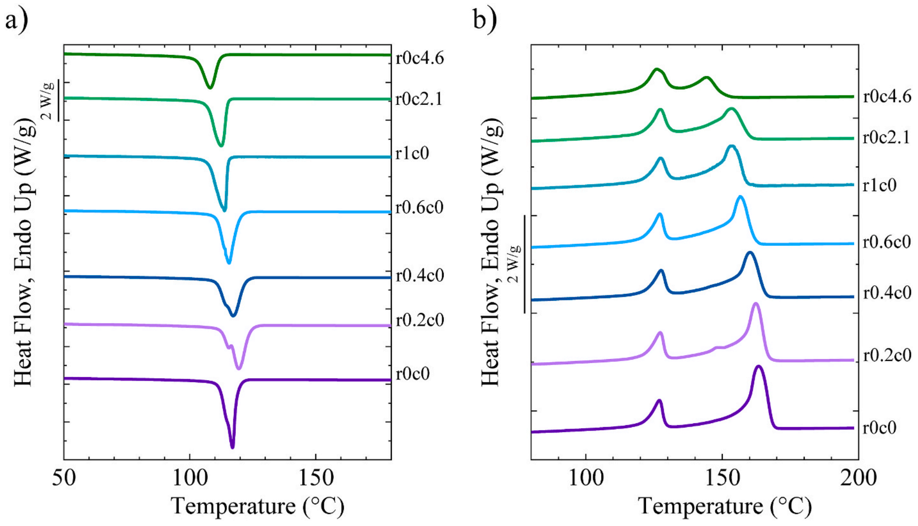

Fig. 3. a) Cooling and b) heating scans of the blends with different regiodefects and comonomer content in the PP phase.

the T_m and T_c of the blends with different regiodefect content, follow the expected trend with intermediate values between the two mixed materials [34–36].

3.3. *Self-nucleation behavior*

The self-nucleation behavior of the blends was studied applying the self-nucleation procedure explained in the experimental section [25–27]. To determine the *self-nucleation Domains* of the sample the cooling scans from T_s and the subsequent heating scans are analysed: as an example the results of r0c0 blend are displayed in Fig. 4. When the r0c0 blend is heated to T_s temperatures equal to 172 °C or above, an isotropic melt is obtained since in the following cooling scan one crystallization peak is obtained and its T_c does not depend on the applied T_s temperature, i.e., T_c is always equal to 117.2 °C. We note that only one peak is observed but a shoulder at 114.6 °C, which corresponds to the PE phase crystallization, is also present. The self-nucleation temperature region above 172 °C is known as *Domain I* of PP. If the T_s temperature is reduced to 170 °C or below two crystallization peaks appear: the largest peak at 123.1 °C corresponds to PP matrix solidification and the small peak at 116.1 °C is related to the PE phase crystallization, which is the minority component. The increase in the T_c of PP indicates that at this temperature some self-seeds were left, which increase the nucleation density and consequently the crystallization kinetics. This temperature range (167–170 °C) corresponds to the self-nucleation *Domain II* of PP. When reducing the T_s to temperatures equal or below 167 °C a progressive increase in the T_c of PP and PE is observed and, most importantly, an additional melting peak at higher temperatures for the PP phase appears in the subsequent heating. This additional T_m corresponds to the melting of small crystal fragment survived at T_s which have annealed and thickened. Thus, at temperatures equal to 167 °C or below the sample is in *Domain III* of PP.

The self-nucleation results can be summarized by considering the melting endotherm obtained when heating from the standard crystalline state, and superposing to this curve the crystallization temperature obtained at each T_s temperature [25–27]. The data corresponding to the r0c0 blends are displayed in Fig. 5a. Above 170 °C a constant crystallization temperature is observed, with PP and PE crystallizing concomitantly, this temperature region corresponds to *Domain I*. Then at temperatures equal or below 170 °C the crystallization peak is split in two, with PP crystallizing at higher temperatures than PE due to the self-seeding. This occurs in *Domain II*. It is worth to note that in the temperature range of *Domain II* there are some self-seeds, rather than self-nuclei, since the DSC endotherm does not reach the baseline [27, 37]. This implies that the sample is in *Domain IIb* since self-seeds or crystal fragments can be present. Thus, for this blend there is no melt memory effect, which is conventionally indicated as that induced by self-nuclei not detected by the DSC (when the endotherm reaches the baseline). When reducing the T_s there is a slight increase of the T_c corresponding to the PE phase. Finally at temperatures equal to 167 °C or below in which annealing of PP phase occurs, in *Domain III*, the T_c of PE reaches a constant value, similarly to the T_c of PP that reaches saturation with respect to T_s. The SN summary results for neat polypropylenes are displayed in the SI (Fig. S2).

The PE in the blend shows an increase in the T_c of almost 3 °C in the 130–170 °C temperature region, which corresponds to *Domain II* and *Domain III* of PP, as can be seen in Fig. 5c. However, the neat PE does not show any significant increase in the T_c in this particular self-nucleation temperature region. Indeed, at high temperatures, neat PE shows a not systematic variation of T_c within 1 °C, until the temperature is reduced to *Domain II* of PE at 130 °C, see Fig. S3. Thus, the increase of the T_c of PE in the blends suggests that surface nucleation of PE onto the PP phase is occurring [9,22,38]. In particular, the trend of T_c for the PE phase is attributed to the increase in the lamellar thickness of the PP matrix with decreasing its self-nucleation temperature, as will be discussed below, which promotes a more efficient surface nucleation of PE.

For the sample with 1 % regiodefects, r1c0, a similar result is observed, with the blend exhibiting *DI*, *DIIb* due to self-seed and *Domain III*, Fig. 5b. Melt memory or *Domain IIa* produced by self-nuclei is absent in this blend. Recently, it has been reported that regiodefects in PP can promote melt memory effect due to the crystallizable sequence partitioning during crystallization, even if they are mainly incorporated within the crystal [39]. However, in the present work the regiodefects do not have a significant effect on melt memory. The regiodefects in the matrix do not prevent the occurrence of PE surface nucleation. The PE T_c in r1c0 increases around 2.5 °C going from PP matrix *Domain I* to *Domain III* (see Fig. 5d), which is similar to the increase observed in the r0c0 blend.

Qualitatively analogous results are shown by the blends containing 2.1 and 4.6 wt% ethylene comonomer, see Fig. S4. Those blends exhibit the three *self-nucleation Domains* including 1 °C of *Domain IIa* or melt memory effect.

Considering all the results of the studied blends, the crystallization temperature of PE phase can be related to the crystallization temperature of the PP matrix, varied through both the self-nucleation process and the changes in the chain microstructure/constitution (Fig. 6). An apparently linear trend between the crystallization temperature of both phases is observed. Interestingly, the data of several blends lay on a

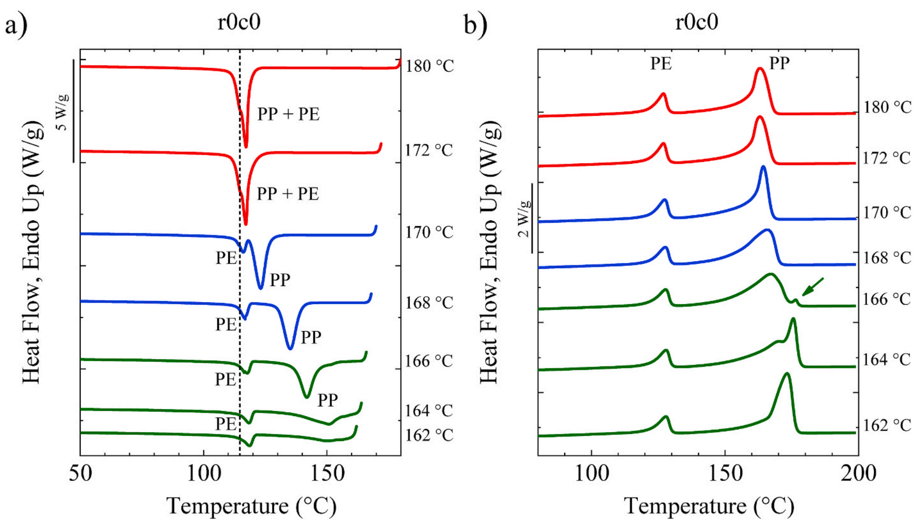

Fig. 4. a) Cooling scans from several T_s temperatures showing the crystallization of PP and PE and b) subsequent heating scans.

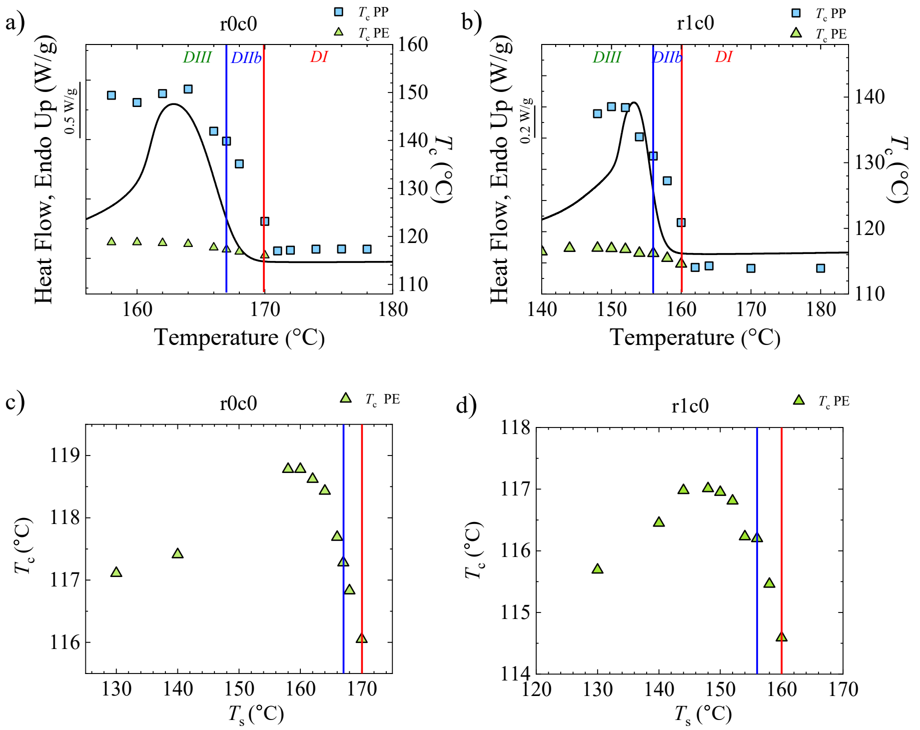

Fig. 5. Self-nucleation results of a) r0c0 and b) r0c1 blends. The black line corresponds to the heating of the sample after a standard crystallization run and the data points indicate the crystallization temperature as a function of T_s. A higher magnification of the plots displaying the trend of the crystallization temperature of polyethylene for c) r0c0 and d) r1c0 is also reported.

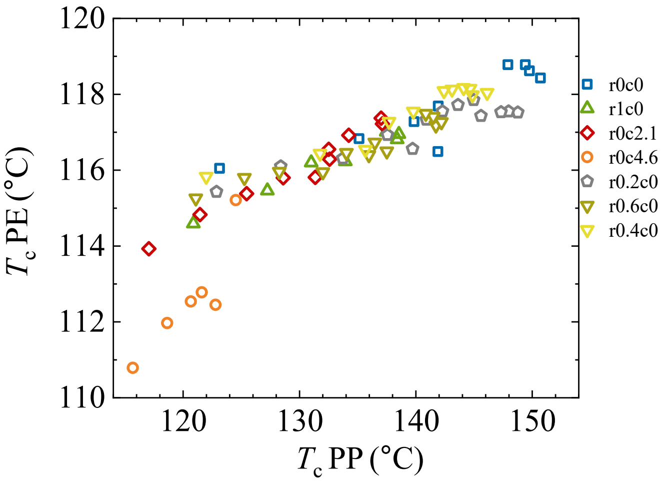

Fig. 6. Crystallization temperature of polyethylene as a function of the crystallization temperature of PP.

single curve, obtaining a master curve, except for the data corresponding to the sample r0c4.6, that has the highest amount of comonomer. As practically all the data superpose, there is a unique slope which implies a single mechanism of nucleation of PE onto the PP phase notwithstanding the PP chain microstructure. Thus, the sensitivity of PE crystallization temperature to the surface induced nucleation of PP depends only on the T_c of the PP matrix. This could be tentatively related to the lamellar thickness of PP, as we know that this morphological parameter is a function of the crystallization temperature. The blend r0c4.6 shows a slightly different slope and much lower values of PE T_c for a given T_c PP. It seems that 4.6 wt% is a high comonomer amount, so the most constitutively defective PP is affecting more significantly the surface nucleation of PE, possibly due to the major differences in the lamellar thickness of the PP phase in this sample compared with the others, as it will be shown later on.

In a previous work from our group, we demonstrated that the regularity of PE chains that form the droplets affects the sensitivity of the PE surface nucleation to the changes in the PP lamellar thickness [22]. In that case different slopes between the T_c of the same PP matrix and the T_c of the different PE droplets were obtained, depending on the chain regularity of PE. More regular PE shows higher T_c values and a more marked response of the crystallization to the variation in the T_c of PP. We concluded that epitaxial crystallization is more efficient for highly regular PE chains. On the other hand, the chain defects hindered the arrangement of PE chains onto PP substrate, reducing the ability of PP to surface nucleate the PE.

3.4. *Lamellar thickness and crystalline structure*

It is assumed that the variation in the crystallization temperature of PP induced by self-seeds or annealed crystals brings to the formation of thicker crystalline lamellae, with decreasing the PP matrix's self-nucleation temperature [40,41]. To gain insight in this relationship, the long period of the different PP matrices has been investigated by SAXS. As an example, in Fig. 7a the SAXS patterns of r0c0 PP matrix crystallized by cooling from several T_s temperatures are displayed. In all the curves a main peak is observed which corresponds to the long period of the material. i.e., the repeating length of the density periodicity comprising the crystalline lamella and the amorphous layer. When the T_s is reduced, a shift to lower q values for the maximum, i.e., a larger long period value, is observed. For the r0c0 blend, the PP matrix enters *Domain II* at 170 °C and *Domain III* at 167 °C. The increase of the long period with T_s below 167 °C correlates well with what expected from the self-nucleation behavior, i.e., a shift to higher crystallization temperature and an annealing, which both lead to thicker lamellae. To verify if self-nucleation has any effect on the crystallinity degree or crystalline phase, Wide-Angle X-ray Scattering (WAXS) measurements were also carried out, see Fig. 7b. For r0c0 the pattern of the monoclinic α-phase

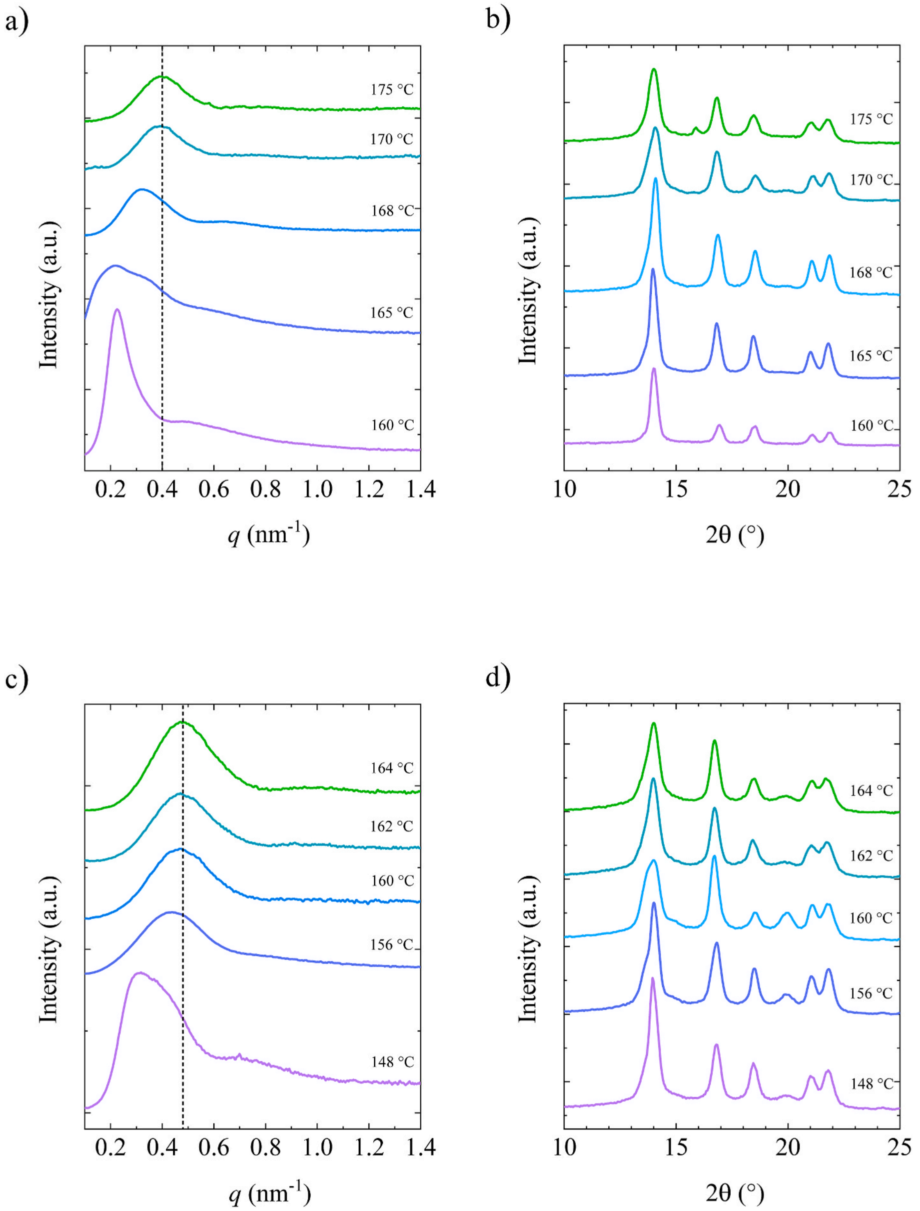

Fig. 7. SAXS and WAXS patterns of PP matrix after crystallizing by cooling from the indicated T_s temperatures: a) SAXS of r0c0, b) WAXS of r0c0, c) SAXS of r1c0, and d) WAXS r1c0.

can be recognized. A minor fraction of γ-polymorph could be individuated [42], especially at the highest self-nucleation temperatures. A magnification around 20° is displayed in the SI, Fig. S5.

A similar trend is observed for the PP which contains 1 % regiodefects. Again, the long period increases when reducing the T_s below 156 °C, Fig. 7c. The WAXS patterns show a majority of α-phase, with a significant fraction of γ-phase (as judged from the peak centered at around 20°), see Fig. 7d. Changing the T_s varies slightly the polymorphic composition, with γ-phase showing a maximum content at around T_s of 156 °C. It has been proved that PP containing regiodefects displays γ-phase [31,32]. The amount of γ-phase increases when cooling from *Domain II* [39]. This is in line with a previous study in which it was demonstrated that reducing the isothermal crystallization temperature the amount of γ-phase increases [31].

The results obtained on the copolymers are included in the SI, Fig. S6. From SAXS experiments, an increase of the long period with reducing T_s is observed, however less significant than the increase for the r0c0 blend. WAXS patterns show that the copolymers contain gamma phase as highlighted by the $(117)_\gamma$ reflection at 20° [42].

The volume crystallinity, X_{CV}, and the long period as a function of the T_s are shown in Fig. 8. The crystallinity degree evaluated from WAXS experiment and corrected for the density of the amorphous and the crystalline phase (i.e., volume-based crystallinity) is calculated according to:

$$X_{CV} = \frac{X_{CW}}{X_{CW} + \frac{\rho_c}{\rho_a}(1 - X_{CW})}$$

X_{CV} being the volume-based crystallinity, X_{CW} the weight-based crystallinity, ρ_a the density of the amorphous phase, and ρ_c the density of the crystalline phase. For PP 0.85 and 0.936 g/cm^3 values were used [43,44].

The results indicate an increase of the crystallinity degree of around 10 % as the self-nucleation temperature is reduced for r0c0 and r1c0. This could be expected considering that via self-nucleation the crystallization process is promoted. This effect is not observed for the PP matrix containing comonomer, so the incorporation of comonomer prevents the

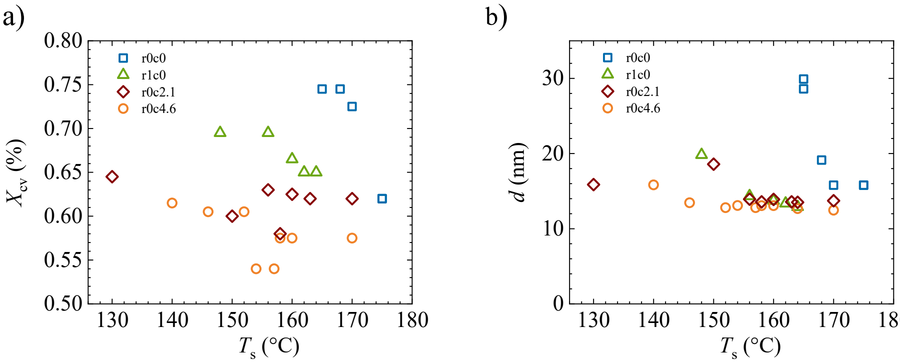

Fig. 8. a) Crystallinity degree and b) long period as a function of self-nucleation temperature for the blends.

increase in crystallinity degree applying low T_s temperatures. Regiodefects and comonomer reduce the crystallinity from 65 % to 53 %. The long period that comprises the crystalline lamellar thickness and amorphous layer shows a similar trend, with an increase at low T_s values, that correspond to *Domain III* in which annealing occurs.

The crystalline lamellar thickness (l_c) has been calculated by multiplying the measured long period for the volume-based crystallinity. The dependence of l_c on crystallization temperature of the various PPs, varied thanks to the self-nucleation procedure, is shown in Fig. 9. In general the lamellar thickness increases with crystallization temperature, less markedly for the materials containing various amount of defects, and more steeply for crystallization temperatures above about 130 °C. The range of lamellar thickness varies from about 5 to roughly 20 nm. Remarkably, the behaviour of all the material can be described by the same trend. The behaviour is in line with the expected increase in the thickness of the lamellae as the crystallization supercooling (in non-isothermal conditions) is decreased [40,41].

At this point, in view of the secondary nucleation theory of polymer-polymer epitaxy proposed by Greso et al. [11], the nucleation of PE, i.e., namely its crystallization temperature, can be correlated to the thickness of the lamellar substrate. Considering that the chain axes of PE and PP are not parallel in the epitaxial nucleation of these polymers, a certain matching between the lamellar sizes of the depositing PE stems and of the PP substrate along the crystallographic matching direction should be fulfilled. For this reason, in Fig. 10 the crystallization temperature of PE, which reflects the efficiency of surface nucleation induced by PP, is plotted against the ratio between $l_{c,PP}$ and the cos(50°), according to Refs. [11–13]. A clear correlation between the two values is found, with the nucleation rate of PE being a direct function of $l_{c,PP}/\cos(50°)$. The average lamellar thickness of PE is also indicated in the plot, by a dashed vertical line. According to the secondary nucleation theory applied to PE/PP epitaxy [11] nucleation can efficiently occur only when $l_{c,PE} < l_{c,PP}/\cos(50°)$. If the opposite would be true, then the PE stems would span more than one PP lamellae and suffer some free energy penalty for the deposition on the PP amorphous layer. Interestingly, from our data, it is seen that for thin PP lamellae a small increase in their thickness results in a strong increase in the PE T_c. This indicates that nucleation of PE can also occur for $l_{c,PE} > l_{c,PP}/\cos(50°)$, hence it can happen across more than one PP lamella. However, if one considers the PE T_c values, this situation determines a lower nucleation efficiency with respect to that obtained for $l_{c,PP}/\cos(50°) > l_{c,PE}$. Regarding the sensitivity of T_c PE with respect to $l_{c,PP}$, this is greater when $l_{c,PE} > l_{c,PP}/\cos(50°)$, since probably PE nucleation is largely affected by the thickness of the PP amorphous layer on which the nucleus must form. Once $l_{c,PP}/\cos(50°)$ reaches the value of $l_{c,PE}$, the increase of T_c PE with $l_{c,PP}$ becomes smaller because a large fraction of PE lamellae can already grow via epitaxy on the thick PP substrate, and the advantage of further increase of $l_{c,PP}$ is no longer significant.

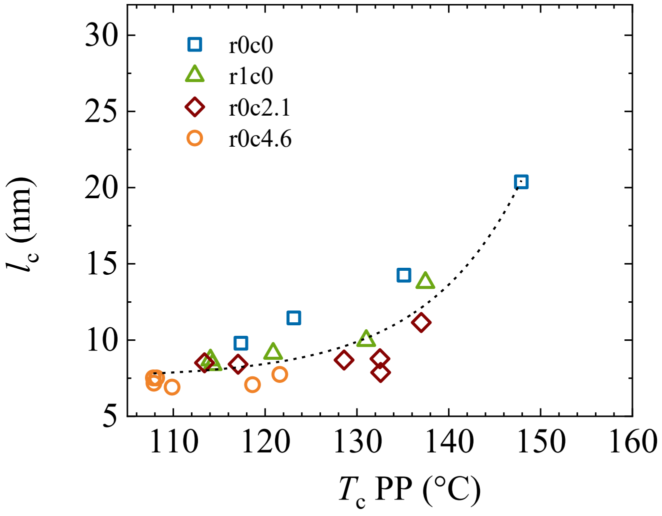

Fig. 9. Crystalline lamellar thickness as a function of non-isothermal T_c of PP, as modified by applying a self-nucleation procedure. The line is a guide to the eyes only.

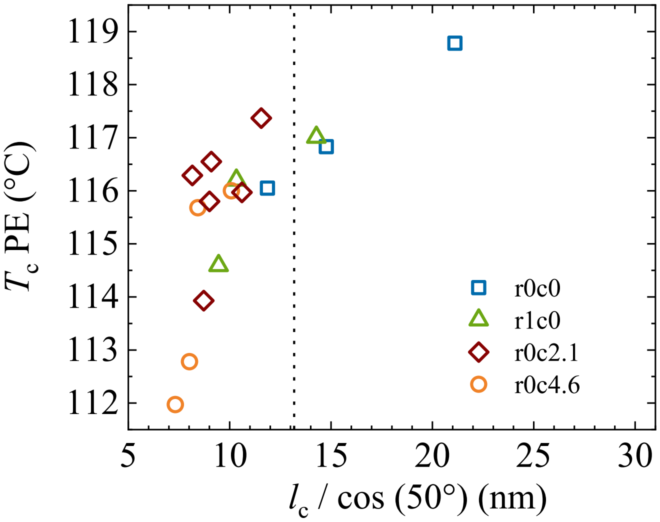

Fig. 10. Crystallization temperature of polyethylene as a function of the crystalline lamellar thickness of PP divided by the cos(50°). The vertical line corresponds to the average crystalline lamellar thickness of polyethylene obtained applying several self-nucleation temperatures.

4. Conclusions

In PP/PE blends, the self-nucleation of PP matrix promotes the surface nucleation of PE droplets. We have recently demonstrated that the regularity of polyethylene chains impacts epitaxy between PE and PP, and that a certain crystallizable sequence length of PE is required to observe the effect. In this work we focus on the role of PP matrix microstructure in the epitaxy of PP/PE blends. PP matrices including varying content of regiodefects or ethylene comonomer are considered. Applying the self-nucleation procedure an increase of the crystallization temperature of PP phase is induced which in turns causes a thickening of PP lamellae. This results in a more efficient surface induced nucleation of PE droplets, as deduced by the increase of crystallization temperature of PE phase. A clear correlation between the crystallization temperature of PE and the lamellar thickness of the PP matrix is established. Both the presence of regiodefects or comonomer impacts the lamellar thickness of PP, so this parameter (l_c) is suitable to capture the role of the PP microstructure. Overall, this work sheds light on the nanoscale morphological parameters of the PP matrix which are involved in the epitaxial crystallization of PE droplets in such polyolefins blends.

CRediT authorship contribution statement

Leire Sangroniz: Writing – review & editing, Writing – original draft, Investigation, Formal analysis, Data curation. **Enrico Carmeli:** Writing – review & editing, Resources, Conceptualization. **Lada Vukusic:** Writing – review & editing, Investigation, Data curation. **Velichko Hristov:** Resources, Investigation. **Martina Galatini:** Investigation. **Davide Tranchida:** Writing – review & editing, Writing – original draft, Funding acquisition, Conceptualization. **Dario Cavallo:** Supervision, Conceptualization.

Declaration of competing Interest

The authors declare that they have no known competing financial interests or personal relationships that could have appeared to influence the work reported in this paper.

Acknowledgements

L.S. acknowledges Margarita Salas fellowship granted by the University of the Basque Country (UPV/EHU) and funded by the European Union-Next Generation EU and the Spanish Government. European Synchrotron Radiation Facility (ESRF) is acknowledged for granting the beamtime number SC-5480.

Appendix A. Supplementary data

Supplementary data to this article can be found online at https://doi.org/10.1016/j.polymer.2025.128144.

Data availability

Data will be made available on request.

References

[1] E. Piorkowska, G.C. Rutledge, Handbook of Polymer Crystallization, John Wiley & Sons, Inc., Hoboken, New Jersey, 2013, https://doi.org/10.1002/9781118541838.

[2] F. Auriemma, G.C. Alfonso, C. De Rosa, Polymer Crystallization I, Springer Cham, Cham, Switzerland, 2017, https://doi.org/10.1007/978-3-319-49203-2.

[3] D. Cavallo, A.J. Müller, Polymer crystallization, in: N. Hadjichristidis, Y. Gnanou, K. Matyjaszewski, M. Muthukumar (Eds.), Macromolecular Engineering, Wiley-VCH GmbH, 2022, https://doi.org/10.1002/9783527815562.mme0032.

[4] J. Xu, G. Reiter, R.G. Alamo, Concepts of nucleation in polymer crystallization, Crystals 11 (2021) 304, https://doi.org/10.3390/cryst11030304.

[5] M. Muthukumar, Nucleation in polymer crystallization, in: S.A. Rice (Ed.), Advances in Chemical Physics, John Wiley & Sons, Inc., Hoboken, New Jersey, 2003, https://doi.org/10.1002/0471484237.ch1.

[6] K.N. Okada, M. Hikosaka, Polymer nucleation, in: E. Piorkowska, G.C. Rutledge (Eds.), Handbook of Polymer Crystallization, John Wiley & Sons, Inc., Hoboken, New Jersey, 2013, https://doi.org/10.1002/9781118541838.ch4.

[7] R. Morales, M. Arnal, A.J. Müller, The evaluation of the state of dispersion in immiscible blends where the minor phase exhibits fractionated crystallization, Polym. Bull. 35 (1995) 379–386, https://doi.org/10.1007/BF00963138.

[8] L. Sangroniz, B. Wang, Y. Su, G. Liu, D. Cavallo, D. Wang, A.J. Müller, Fractionated crystallization in semicrystalline polymers, Prog. Polym. Sci. 115 (2021) 101376, https://doi.org/10.1016/j.progpolymsci.2021.101376.

[9] E. Carmeli, S.E. Fenni, M.R. Caputo, A.J. Müller, D. Tranchida, D. Cavallo, Surface nucleation of dispersed polyethylene droplets in immiscible blends revealed by polypropylene matrix self-nucleation, Macromolecules 54 (2021) 9100–9112, https://doi.org/10.1021/acs.macromol.1c01430.

[10] S.E. Fenni, A.J. Müller, D. Cavallo, Understanding polymer nucleation by studying droplets crystallization in immiscible polymer blends, Polymer 264 (2023) 125514, https://doi.org/10.1016/j.polymer.2022.125514.

[11] A.J. Greso, P.J. Phillips, The role of secondary nucleation in epitaxial growth: the template model, Polymer 35 (1994) 3373–3376, https://doi.org/10.1016/0032-3861(94)90897-4.

[12] Shouke Yan, Jürgen Petermann, Decai Yang, Effect of lamellar thickness on the epitaxial crystallization of PE on oriented iPP films, Polym. Bull. 38 (1997) 87–94, https://doi.org/10.1007/s002890050023.

[13] Shouke Yan, Decai Yang, Jürgen Petermann, Controlling factors for the occurrence of heteroepitaxy of polyethylene on highly oriented isotactic polypropylene, Polymer 39 (19) (1998) 4569–4578, https://doi.org/10.1016/S0032-3861(97)10137-9.

[14] R. Xin, J. Zhang, X. Sun, H. Li, Z. Qiu, S. Yan, Epitaxial effects on polymer crystallization, in: F. Auriemma, G.C. Alfonso, C. de Rosa (Eds.), Polymer Crystallization II, Advances in Polymer Science, vol. 277, Springer, Cham, 2015, https://doi.org/10.1007/12_2015_329.

[15] A. Thierry, B.A. Lotz, Epitaxial crystallization of polymers: means and issues, in: E. Piorkowska, G.C. Rutledge (Eds.), Handbook of Polymer Crystallization, John Wiley & Sons, Inc., Hoboken, New Jersey, 2013, https://doi.org/10.1002/9781118541838.ch8.

[16] C. Hou, J. Wang, P. Wang, J. Cui, S. Wang, R. Xin, H. Li, X. Sun, Z. Ren, S. Yan, Epitaxy-Directed self-assembly of copolymers and polymer blends, Adv. Sci. 11 (2024) 2207707, https://doi.org/10.1002/advs.202207707.

[17] M. Zhou, D. Mi, F. Hou, J. Zhang, Insight into understanding the evolution of the epitaxy crystallization in isotactic polypropylene and polyethylene blends, Polym. Adv. Technol. 28 (2017) 1750–1758, https://doi.org/10.1002/pat.4052.

[18] B. Na, Q. Zhang, K. Wang, L. Li, Q. Fu, Origin of various lamellar orientations in high-density polyethylene/isotactic polypropylene blends achieved via dynamic packing injection molding: bulk crystallization vs. epitaxy, Polymer 46 (2005) 819–825, https://doi.org/10.1016/j.polymer.2004.11.110.

[19] P. Deng, B. Whiteside, F. Wang, K. Norris, J. Zhang, Epitaxial growth and morphological characteristics of isotactic polypropylene/polyethylene blends: scale effect and mold temperature, Polym. Test. 34 (2014) 192–201, https://doi.org/10.1016/j.polymertesting.2014.01.006.

[20] R. Su, K. Wang, P. Zhao, Q. Zhang, R. Du, Q. Fu, L. Li, L. Li, Shear-induced epitaxial crystallization in injection-molded bars of high-density polyethylene/isotactic polypropylene blends, Polymer 48 (2007) 4529–4536, https://doi.org/10.1016/j.polymer.2007.06.001.

[21] B. Na, K. Wang, P. Zhao, Q. Zhang, R. Du, Q. Fu, Z. Yu, E. Chen, Epitaxy growth and directed crystallization of high-density polyethylene in the oriented blends with isotactic polypropylene, Polymer 46 (2005) 5258–5267, https://doi.org/10.1016/j.polymer.2007.06.001.

[22] M. Góra, S. Coba-Daza, E. Carmeli, D. Tranchida, A. Albrecht, A.J. Müller, D. Cavallo, Surface-enhanced nucleation in immiscible polypropylene and polyethylene blends: the effect of polyethylene chain regularity, Polymer 282 (2023) 126180, https://doi.org/10.1016/j.polymer.2023.126180.

[23] Nydenm VanderHart, Alamo, et al., Abstr. Pap. Am. Chem. Soc. 219 (2000 Mar 26) 48–PMSE.

[24] M. Gahleitner, J.R. Severn, Designing polymer properties, in: Tailor-Made Polymers: via Immobilization of Alpha-Olefin Polymerization Catalysts, vols. 1–42, 2008.

[25] B. Fillon, J. Wittmann, B. Lotz, A. Thierry, Self-nucleation and recrystallization of isotactic polypropylene (α phase) investigated by differential scanning calorimetry, J. Polym. Sci., Part B: Polym. Phys. 31 (1993) 1383–1393, https://doi.org/10.1002/polb.1993.090311013.

[26] R. Michell, A. Mugica, M. Zubitur, A.J. Müller, Self-nucleation of crystalline phases within homopolymers, polymer blends, copolymers, and nanocomposites, in: F. Auriemma, G.C. Alfonso, C. De Rosa (Eds.), Polymer Crystallization I, Springer Cham, Cham, Switzerland, 2017, https://doi.org/10.1007/12_2015_327.

[27] L. Sangroniz, D. Cavallo, A.J. Müller, Self-nucleation effects on polymer crystallization, Macromolecules 53 (2020) 4581–4604, https://doi.org/10.1021/acs.macromol.0c00223.

[28] B. Chu, B.S. Hsiao, Small-angle X-ray scattering of polymers, Chem. Rev. 101 (2001) 1727–1762, https://doi.org/10.1021/cr9900376.

[29] G. Ochbaum, R. Bitton, Using small-angle X-ray scattering (SAXS) to study the structure of self-assembling biomaterials, in: H.S. Azevedo, R.M.P. da Silva (Eds.), Self-assembling Biomaterials, Woodhead Publishing, UK, 2018, https://doi.org/10.1016/B978-0-08-102015-9.00015-0.

[30] N. Stribeck, X-Ray Scattering of Soft Matter, Springer Berlin, Heidelberg, 2007, https://doi.org/10.1007/978-3-540-69856-2.

[31] C. De Rosa, F. Auriemma, A. Di Capua, L. Resconi, S. Guidotti, I. Camurati, E. I. Nifant'ev, I.P. Laishevtsev, Structure− property correlations in polypropylene from metallocene catalysts: stereodefective, regioregular isotactic polypropylene, J. Am. Chem. Soc. 126 (2004) 17040–17049, https://doi.org/10.1021/ja045684f.

[32] D. Tranchida, L. Resconi, Influence of 2, 1-erythro regiodefects on the crystallization behavior of isotactic polypropylene, Polymer Crystallization 1 (2018) e10022, https://doi.org/10.1002/pcr2.10022.

[33] C. Paulik, C. Tranninger, J. Wang, P. Shutov, D. Mileva, M. Gahleitner, Catalyst type effects on structure/property relations of polypropylene random copolymers, Macromol. Chem. Phys. 222 (2021) 2100302, https://doi.org/10.1002/macp.202100302.

[34] Y.C. Shu, K.J. Hsiao, W.C. Tsen, Thermal characteristics and crystallinity of Ziegler–Natta isotactic polypropylene/metallocene isotactic polypropylene polyblended fibers, J. Appl. Polym. Sci. 113 (2009) 265–273, https://doi.org/10.1002/app.30122.

[35] C. Dong, H. Niu, J.Y. Dong, "Two-in-One" catalysis of broad/bimodal molecular-weight-distribution polypropylene by a combination of Ziegler–Natta and metallocene catalysts, Appl. Catal. Gen. 484 (2014) 142–147, https://doi.org/10.1016/j.apcata.2014.07.019.

[36] A. Lisovskii, M. Shuster, M. Gishvoliner, G. Lidor, M.S. Eisen, Polymerization of propylene by metallocene and Ziegler–Natta mixed catalytic systems. Study of polypropylene properties, J. Polym. Sci. Polym. Chem. 36 (1998) 3063–3072, https://doi.org/10.1002/(SICI)1099-0518(199812)36:17<3063::AID-POLA7>3.0.CO;2-2.

[37] L. Sangroniz, R.G. Alamo, D. Cavallo, A. Santamaria, A.J. Müller, A. Alegría, Differences between isotropic and self-nucleated PCL melts detected by dielectric experiments, Macromolecules 51 (2018) 3663–3671, https://doi.org/10.1021/acs.macromol.8b00708.

[38] E. Carmeli, G. Kandioller, M. Gahleitner, A.J. Müller, D. Tranchida, D. Cavallo, Continuous cooling curve diagrams of isotactic-polypropylene/polyethylene blends: mutual nucleating effects under fast cooling conditions, Macromolecules 54 (2021) 4834–4846, https://doi.org/10.1021/acs.macromol.1c00699.

[39] A. Cicolella, C. De Rosa, E. Sepe, F. De Stefano, A. Giordano, M. Scoti, The impact of regiodefects on the melt-memory of isotactic polypropylene, Macromol. Rapid Commun. 45 (2024) 2400233, https://doi.org/10.1002/marc.202400233.

[40] K. Mezghani, R. Anderson Campbell, P.J. Phillips, Lamellar thickening and the equilibrium melting point of polypropylene, Macromolecules 27 (1994) 997–1002, https://doi.org/10.1021/ma00082a017.

[41] P. Maiti, M. Hikosaka, K. Yamada, A. Toda, F. Gu, Lamellar thickening in isotactic polypropylene with high tacticity crystallized at high temperature, Macromolecules 33 (2000) 9069–9075, https://doi.org/10.1021/ma012498a.

[42] C. De Rosa, F. Auriemma, M. Paolillo, L. Resconi, I. Camurati, Crystallization behavior and mechanical properties of regiodefective, highly stereoregular isotactic polypropylene: effect of regiodefects versus stereodefects and influence of the molecular mass, Macromolecules 38 (2005) 9143–9154, https://doi.org/10.1021/ma051004x.

[43] N.P. Cheremisinoff, Condensed Encyclopedia of Polymer Engineering Terms, Butterworth-Heinemann, Oxford, UK, 2001.

[44] A.T. Lorenzo, M.L. Arnal, J. Albuerne, A.J. Müller, DSC isothermal polymer crystallization kinetics measurements and the use of the Avrami equation to fit the data: guidelines to avoid common problems, Polym. Test. 26 (2007) 222–231, https://doi.org/10.1016/j.polymertesting.2006.10.005.